WATER RESOURCES RESEARCH, VOL. 49, 3165–3179, doi:10.1002/wrcr.20176, 2013

Estimation of river depth from remotely sensed hydraulic relationships

Matthew K. Mersel,[1,2] Laurence C. Smith,[1,3] Konstantinos M. Andreadis,[4] and Michael T. Durand[5,6]

Received 13 October 2012; revised 26 February 2013; accepted 2 March 2013; published 4 June 2013.

[1] The Surface Water and Ocean Topography (SWOT) radar interferometer satellite mission will provide unprecedented global measurements of water surface elevation (h) for inland water bodies. However, like most remote sensing technologies SWOT will not observe river channel bathymetry below the lowest observed water surface, thus limiting its value for estimating river depth and/or discharge. This study explores if remotely sensed observations of river inundation width and h alone, when accumulated over time, may be used to estimate this unmeasurable flow depth. To test this possibility, synthetic values of h and either cross-sectional flow width (w) or effective width (W_e, inundation area divided by reach length) are extracted from 1495 previously surveyed channel cross-sections for the Upper Mississippi, Illinois, Rio Grande, and Ganges-Brahmaputra river systems, and from 62 km of continuously acquired sonar data for the Upper Mississippi. Two proposed methods (called "Linear" and "Slope-Break") are tested that seek to identify a small subset of geomorphically "optimal" locations where w or W_e covary strongly with h, such that they may be usefully extrapolated to estimate mean cross-sectional flow depth (d). While the simplest Linear Method is found to have considerable uncertainty, the Slope-Break Method, identifying locations where two distinct hydraulic relationships are identified (one for moderate to high flows and one for low flows), holds promise. Useful slope breaks were discovered in all four river systems, ranging from 6 (0.04%) to 242 (16%) of the 1495 studied cross-sections, assuming channel bathymetric exposures ranging from 20% to 95% of bankfull conditions, respectively. For all four rivers, the derived depth estimates from the Slope-Break Method have root mean squared errors (RMSEs) of $<$20% (relative to bankfull mean depth) assuming at least one channel bathymetry exposure of $\sim$25% or greater. Based on historic discharge records and HEC-RAS hydraulic modeling, the Upper Mississippi and Rio Grande rivers experience adequate channel exposures at least $\sim$60% and $\sim$42% of the time, respectively. For the Upper Mississippi, so-called "reach-averaging" (spatial averaging along some predetermined river length) of native-resolution h and W_e values reduces both RMSE and longitudinal variability in the derived depth estimates, especially at reach-averaging lengths of $\sim$1000–2000 m. These findings have positive implications for SWOT and other sensors attempting to estimate river flow depth and/or discharge solely from incomplete, remotely sensed hydraulic variables, and suggest that useful depth retrievals can be obtained within the spatial and temporal constraints of satellite observations.

Citation: Mersel, M. K., L. C. Smith, K. M. Andreadis, and M. T. Durand (2013), Estimation of river depth from remotely sensed hydraulic relationships, *Water Resour. Res.*, *49*, 3165–3179, doi:10.1002/wrcr.20176.

[1]Department of Geography, University of California, Los Angeles, California, USA.
[2]Now at U.S. Army Cold Regions Research and Engineering Laboratory (CRREL), Hanover, New Hampshire, USA.
[3]Department of Earth and Space Sciences, University of California, Los Angeles, California, USA.
[4]Jet Propulsion Laboratory, California Institute of Technology, Pasadena, California, USA.
[5]School of Earth Sciences, The Ohio State University, Columbus, Ohio, USA.
[6]The Byrd Polar Research Center, The Ohio State University, Columbus, Ohio, USA.

Corresponding author: M. K. Mersel, Cold Regions Research and Engineering Laboratory, RS/GIS 103, 72 Lyme Rd., Hanover, NH 03755, USA. (mmersel@ucla.edu)

©2013. American Geophysical Union. All Rights Reserved.
0043-1397/13/10.1002/wrcr.20176

1. Introduction

[2] Terrestrial runoff to rivers is a significant term in the global water balance and a principle source of fresh water for human and ecosystem use [*Vörösmarty et al*., 2010], yet global knowledge of the spatial and temporal dynamics of river flow is surprisingly poor [*Alsdorf et al*., 2007b; *Durand et al*., 2010a]. Stream gages, the traditional method for measuring discharge, are in decline globally [*Stokstad*, 1999; *Shiklomanov et al*., 2002], and where gages do exist, these data are not always shared among countries or agencies. Furthermore, gages are inherently limited to providing information only at single points along a river and fail to capture three-dimensional dynamics of fluvial systems including overbank flow, flood waves, and multichannel flow. These limitations, combined with rising worldwide

stress on river systems owing to industrialization, population growth, and climate change [*United Nations Educational, Scientific and Cultural Organization*, 2012], motivate development of new approaches for understanding river dynamics from satellite observations that would compliment ground-based measurements.

[3] Remote sensing of rivers is a relatively immature but rapidly emerging subdiscipline within hydrology that is advancing new approaches to the study of fluvial systems [*Smith*, 1997; *Alsdorf et al*., 2007b; *Durand et al*., 2010a; *Marcus and Fonstad*, 2010]. Furthermore, the unique spatial perspective afforded from satellite and aircraft sensors allows for observation and understanding of rivers in ways both infeasible and fundamentally different from traditional ground-based methods. One approach is the use of profiling oceanographic radar altimeters to retrieve measurements of water surface elevation (h) along transects where orbit paths cross water bodies [e.g., *Koblinsky et al*., 1993; *Birkett*, 1998; *Birkett et al*., 2002; *Frappart et al*., 2005; *Crétaux and Birkett*, 2006; *Calmant et al*., 2008; *Birkett and Beckley*, 2010; *Lee et al*., 2011]. However, such techniques are generally limited to lakes, reservoirs, and very large rivers and, like stream gages, are inherently point based. Other studies have mapped spatial variations in river inundation area (A) as a proxy for changing stage or discharge, using visible/near-infrared or synthetic aperture radar (SAR) backscatter imagery [e.g., *Smith et al*., 1995, 1996; *Prigent et al*., 2001; *Brakenridge et al*., 2005; *Papa et al*., 2006; *Smith and Pavelsky*, 2008; *Khan et al*., 2011]. However, these methods typically require ancillary data (e.g., from stream gages or digital elevation models (DEMs)) and are most effective for rivers where discharge fluctuations are accommodated largely by width adjustments (e.g., braided rivers and overbank flows in floodplain systems). Furthermore, cloud and vegetation cover limits the use of optical sensors, while SAR backscatter techniques are limited by difficulties related to wind roughening of the water surface [*Smith*, 1997].

[4] The preceding approaches measure either point-based h, or spatially varying A, but not both. An exciting development in satellite remote sensing of river hydraulics is 3-D imaging, first advanced using repeat-pass interferometric SAR (InSAR) to measure relative changes in h over time and space [e.g., *Alsdorf et al*., 2000, 2001, 2007a; *Lu et al*., 2005; *Jung and Alsdorf*, 2010; *Jung et al*., 2010]. This particular method can detect temporal changes in h to a vertical precision of centimeters, but requires inundated woody vegetation for signal return and only measures relative changes (i.e., height anomalies, $\mathrm{d}h/\mathrm{d}t$) over time, not h. Hydraulic surface slopes, therefore, cannot be mapped with this method. Furthermore, while repeat-pass InSAR demonstrates the vast potential of remote sensing for studying 3-D river dynamics, no sensor currently exists to quantify terrestrial surface water elevations, storages, and fluxes globally over time and space [*Alsdorf et al*., 2007b; *Durand et al*., 2010b].

[5] The Surface Water and Ocean Topography (SWOT) satellite, a joint project between NASA and the French space agency, the Centre National d'Etudes Spatiales (CNES), is planned for launch in 2020 and has strong potential to overcome many of the aforementioned limitations (http://swot.jpl.nasa.gov). SWOT will use a Ka-band interferometric wide-swath altimeter, to provide unprecedented measurements of terrestrial and ocean water surface elevations globally with high spatial resolution. Through instantaneous detection of both h and A, SWOT will acquire repeated DEMs of terrestrial water surfaces wider than ~100 m. Repeat-pass measurements of h and A will essentially map any exposed portion of a river channel's bathymetry between the highest and lowest water surfaces encountered over time. Additionally, topographic mapping of fully exposed river bathymetry (i.e. any portion of the river channel that happens to be fully dry at the time of one or more satellite overpasses) and adjacent floodplains will be achieved using standard interferometric techniques (in the case of SWOT, multiple overpasses would likely be required due to lower signal-to-noise ratio over land). Owing to the very bright returns of near-nadir Ka band radar over water, instantaneous measurements of A, h, and water surface slope will be obtained globally at least once every 11 days, and near-daily at high latitudes.

[6] While global satellite measurements of A, h and water surface slope ($\mathrm{d}h/\mathrm{d}x$) will have numerous scientific and practical applications, they do not permit direct calculation of river discharge (m^3/s). Global knowledge of river discharge would, for instance, greatly improve knowledge of the availability and fluxes of surface water, especially in remote or developing regions where few river gages exist. However, unless the full channel bathymetry is either independently known or is adequately observed over the SWOT mission lifetime (i.e., the river is repeatedly imaged while completely dry), the depth of river flow below the lowest observed h will remain unknown. This unknown residual flow depth is a critical obstacle to estimating river discharge using SWOT and other satellite technologies.

[7] Alternate approaches for remote sensing of river depth are few in number. Several studies have exploited the attenuation of bottom reflectance in the water column using optical imagery [e.g., *Legleiter et al*., 2004, 2009; *Marcus and Fonstad*, 2008; *Legleiter and Roberts*, 2009], but spectral scattering from suspended solids limits this approach to clear, shallow streams where the channel bottom can be seen. Others have used data assimilation techniques to combine simulated observations of h with a hydrodynamic model to solve for depth and discharge simultaneously [e.g., *Andreadis et al*., 2007; *Durand et al*., 2008; *Biancamaria et al*., 2011], while another method [*Durand et al*., 2010b] estimates stream depth using an algorithm based on the Manning equation. Although these last two approaches show considerable promise, limitations of such model-based approaches include their computational expense and reliance on parameterization data that are not always available.

[8] Few studies have explored the river depth-estimation problem from a purely empirical standpoint. Using a large data set compiled from U.S. Geological Survey cross-sections, *Bjerklie* [2007] developed a simple regression equation to estimate bankfull mean depth (d_{bf}, the mean depth at bankfull discharge) from observed values of bankfull width and channel slope. This equation produced a large standard error of ~58%, leading the authors to call for "improved methods to estimate bankfull depth from observed variables" [*Bjerklie*, 2007].

[9] One such method could be to exploit empirical relationships between covarying, interrelated hydraulic variables

(e.g., width w, depth d, and velocity v), where stable relationships exist, to estimate one variable (i.e., d) using another. Identification of these empirical relationships has been a central theme in fluvial geomorphology for decades, both at single locations (called "at-a-station hydraulic geometry (HG)") and longitudinally along a river ("downstream HG"). Classic HG theory formulates the empirical relationships of w, d, and v with discharge (Q), expressed as the simple power functions $w=aQ^b$, $d=cQ^f$, and $v=kQ^m$, where *a, b, c, f, k, and m* are empirical constants unique to a particular river or cross-section and determined through accumulation of field measurements [*Leopold and Maddock*, 1953]. Because $Q=wdv$, the exponents b, f, and m describe the "trade-offs" between flow width, depth, and velocity (i.e., $b+f+m=1$), controlled mainly by the unique bathymetric shape of a stream channel at a given location (for at-a-station HG). Indeed, where stable at-a-station HG relationships exist, they form the basis for traditional stream gage discharge estimates, through construction of an empirical h-Q relationship (rating curve) correlating continuous measurements of h to occasional in situ measurements of Q. For locations where discharge adjustments are depth sensitive (i.e., changes in Q are significantly accommodated by adjustments in depth) and for flows confined within the channel banks, h thus becomes a reliable proxy for discharge.

[10] Stable at-a-station HG relationships have long been observed in field measurements, and it now appears possible to also detect them from space [*Smith and Pavelsky*, 2008]. This suggests that remotely sensed A (or more properly remotely sensed "effective width" W_e, which is A divided by some defined reach length, *Smith et al*. 1995, 1996) and h, such as will be acquired by SWOT, will be useful for estimating certain hydraulic properties of river channels. In particular, for those locations along a river where a stable relationship between h and W_e is detected in satellite observations accumulated over a range of flow conditions, this relationship might then be extrapolated to the unobserved portion of the river channel to estimate the lowest channel bed elevation ($z_{\min}$), from which mean flow depth d is easily computed.

[11] In principle, even discharge Q could be estimated if all of the necessary HG coefficients can be determined. A key uncertainty in adapting at-a-station HG to the remote sensing context, however, is that numerous studies have shown that HG coefficients are highly variable along natural river courses [e.g., *Leopold and Maddock*, 1953; *Richards*, 1973; *Knighton*, 1975; *Park*, 1977] meaning that such functions are site specific and not transferable to other locations. Furthermore, this heterogeneity introduces the key question of how empirical HG relationships, traditionally obtained only at surveyed river cross-sections, are influenced by "reach-averaging" (spatial averaging over some defined reach length) that is inherently necessary using remote-sensing technologies [*Smith and Pavelsky*, 2008]. SWOT radar echoes, in particular, must be spatially averaged over reach lengths of hundreds to thousands of meters (depending on the width of the river or water body) in order to improve their associated measurement precisions of h [*Durand et al*., 2010a]. The implications of this level of reach-averaging on empirical HG relationships are not well understood, with a bare handful of studies examining this question to date [*Stewardson*, 2005; *Smith and Pavelsky*, 2008; *Fonstad and Marcus*, 2010].

[12] Even at a single cross-section, temporal variability in HG relationships is common, particularly when comparing high- versus low-flow conditions [*Lewis*, 1966; *Richards*, 1976; *Phillips*, 1990; *Jowett*, 1998]. Indeed, *Lewis* [1966] highlights substantial "slope breaks" in HG power-law relationships that often occur at low flows, suggesting that remotely sensed HG relationships calibrated at moderate to high flow levels would thus lead to large errors if extrapolated to low flows. Instead of a single empirical function existing relating each hydraulic variable (w, d, and v) to discharge, his study found that in-channel HG relationships are often best described by two functions, one for moderate to high flows and one for low flows [*Lewis*, 1966]. Similarly, from a remote sensing perspective, a W_e-h relationship derived from satellite observations during moderate to high flows might be expected to lead to large errors if extrapolated to estimate river depth d. If a low-flow W_e-h relationship could be detected, however (again, from many observations of W_e and h accumulated over time), its extrapolation might be better suited for estimating d.

[13] The objective of this study is to explore the feasibility of estimating unobservable mean depth d (either cross-sectional mean depth or reach-averaged mean depth) from remotely sensed measurements of water surface elevation h, cross-sectional flow width w, or reach-scale effective width W_e alone. To do this, we extract synthetic values of h, and w from 1495 field surveyed river cross-sections compiled for the Ganges-Brahmaputra, Rio Grande, Illinois, and Upper Mississippi river systems; and values of h and W_e from a sonar-derived, continuously gridded (5 m resolution) bathymetric data set for an overlapping 62 km reach of the Upper Mississippi. For the Rio Grande and Upper Mississippi rivers only, synthetic values of h and w are also generated using the U.S. Army Corps of Engineers (USACE) Hydraulic Engineering Center—River Analysis System 1-D hydraulic model (HEC-RAS) version 4.1.0 (http://www.hec.usace.army.mil/software/hec-ras/), thus allowing the results for these two rivers to also be presented in terms of temporal discharge exceedance probability [*Dingman*, 1994]. While an essentially unlimited number of channel geometries exist in nature, preliminary assessment of the acquired cross-section and bathymetry data sets revealed two simple recurring relationships between w (or W_e) and h. These two w-h (or W_e-h) relationships were found in all five data sets to varying degrees despite substantial differences with respect to channel geometry, location, and river type. Based on this preliminary assessment of the data, the generated data sets of w versus h (or W_e versus h) are then used to test two methods for estimating d by exploiting these two simple satellite-observable w-h relationships. The "Linear Method" extrapolates w-h or W_e-h relationships to estimate d only for those locations where a single, strongly linear correlation between these two variables is observed, across a range of different channel exposures (i.e., down to some minimum low-flow h). The "Slope-Break Method", motivated by *Lewis* [1966], extrapolates w versus h (or W_e versus h) relationships to estimate d only for those locations where two strongly linear correlations are observed, one for moderate to high flows and one for low flows. Both methods are then assessed as to the abundance of locations identified and the corresponding quality of their extrapolated depth estimates. Finally, the influence of reach-averaging is examined using the continuously

gridded sonar data set for the upper Mississippi River, to examine a range of spatially averaged W_e-h relationships that could realistically be sampled by SWOT or other imaging remote sensing technologies.

2. Methods

2.1. Data and Study Areas

[14] A total of 1495 previously acquired field-survey cross-sections were compiled from various sources for six tributary rivers of the Ganges-Brahmaputra system, Bangladesh (http://www.iwmbd.org), and reaches of the Rio Grande River, USA [*Tetra Tech Inc*., 2005], Illinois River, USA [*U.S. Army Corps of Engineers*, 2004], and Upper Mississippi River, USA [*U.S. Army Corps of Engineers*, 2004]. Additionally, continuous gridded bathymetric data overlapping ~62 km of the Upper Mississippi cross-section data set were obtained (http://www.umesc.usgs.gov/aquatic/bathymetry/download.html). Viewed collectively, these four study areas represent a wide range of rivers in terms of their size (~50–18,000 m wide) and discharge (~1–50,000 m/s^3). The locations of these data sets and study areas are shown in Figure 1. The total number of cross-sections, as well as the minimum, mean, and maximum values of bankfull width (w_{bf}) and bankfull mean depth (d_{bf}) for each of the five data sets acquired are listed in Table 1.

[15] Each cross-section in the compiled database consists of a single transect of x and z values (distance perpendicular to the direction of flow and distance above sea level, respectively) surveyed at a particular location along the river. For the Ganges-Brahmaputra system, a total of 224 cross-sections were surveyed by the Bangladesh Institute of Water Modeling (IWM) along seven tributary rivers (Brahmaputra, Ganges, Jamuna, Padma, Surma, Upper Meghna, and Lower Meghna rivers) (Figure 1). This river system constitutes one of the largest in the world, with a mean discharge of ~40,000 m^3/s and channel widths occasionally exceeding 10 km. Much of it is anastomosing, with wide, multithreaded channels interspersed with permanent and shifting islands. For the Rio Grande River, a total of 150 cross-sections were surveyed by Tetra Tech, Inc. along ~172 km from the Caballo Dam in southern New Mexico to the American Dam near the U.S./Mexico border (Figure 1). This part of the Rio Grande is a semiarid environment, surrounded primarily by farmland, and regulated by the upstream Caballo Dam and reservoir. Mean discharge is ~20 to 30 m^3/s with channel widths ranging from ~30 to 130 m. For the Illinois River, 482 cross-sections were surveyed along ~338 km by the USACE, in an area of temperate climate, surrounded mostly by farmland, and regulated by a series of locks and dams. Mean discharge down this reach increases from approximately ~280 to 1000 m^3/s, with channel widths ranging from ~70 to 3300 m. For the Upper Mississippi, a total of 639 cross-sections were surveyed by the USACE over ~315 km, upstream of its confluence with the Ohio River. The Upper Mississippi lies in an area of temperate climate, is surrounded largely by farmland, and is also regulated by a series of locks and dams. Discharge along this reach averages between ~6000 and 7000 m^3/s and channel widths range from ~200 to 2300 m. An overlapping, continuously gridded (5 m × 5 m) bathymetric data set, obtained primarily from depth soundings and supplemented with manual measurements using a calibrated sounding pole was also obtained for a ~62 km river reach of this site. This continuously gridded bathymetric data set was adjusted to a constant reference water surface by the developers of the data set, thus removing water surface slope while preserving the shape of the channel [*Rogala*, 1999]. While a comprehensive assessment of the accuracies of these data sets and of the data collection techniques used to derive them is beyond the scope of this study, accuracies are those typically associated with ADCP, LiDAR, and sonar measurements.

2.2. Extraction of Synthetic Width and h Values

[16] Synthetic values of water surface width w (for cross-sections) and effective width W_e (for the gridded Upper Mississippi data) and h were extracted to test two

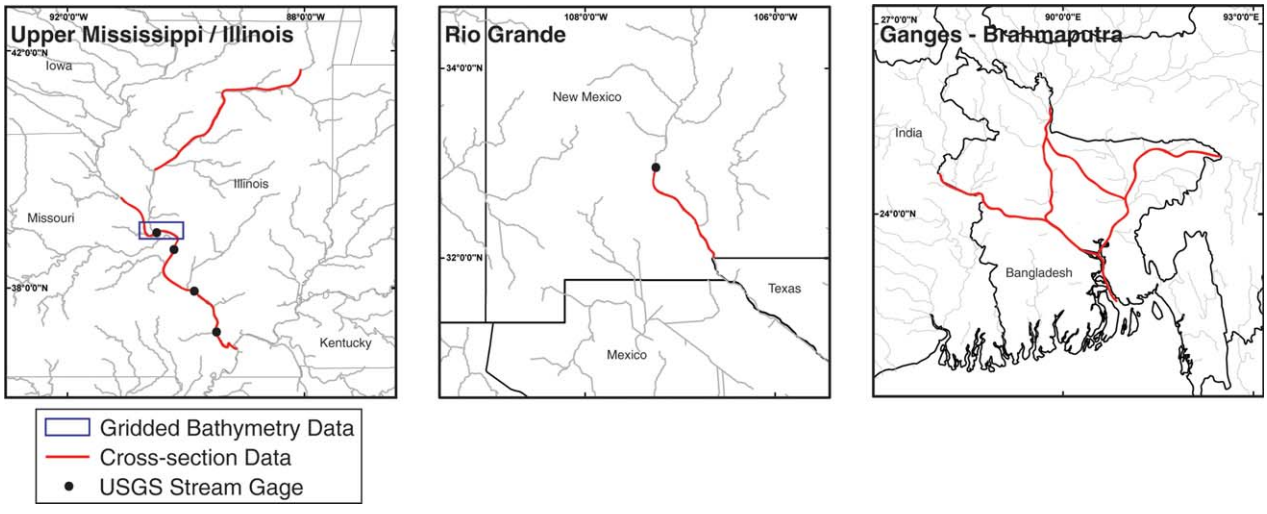

Figure 1. Location map of study areas and field data sets. 1495 intermittent surveyed cross-sections were obtained from various sources along those river reaches highlighted in red. Blue box highlights a ~62km reach of the Upper Mississippi for which gridded bathymetric data were also acquired. Black symbols mark the locations of USGS stream gages used for calculation of discharge statistics.

Table 1. Total Number of Cross-Sections, and Minimum, Mean, and Maximum Values of Bankfull Width (w_{bf}) and Bankfull Mean Depth (d_{bf}) From Each of Four River Cross-Section Data Sets and One Gridded Bathymetric Data Set

River	Number of cross-sections	Min. w_{bf}	Mean w_{bf}	Max. w_{bf}	Min. d_{bf}	Mean d_{bf}	Max. d_{bf}
Upper Mississippi	639	240.89	798.37	2313.01	2.20	7.30	12.69
Illinois	482	73.81	414.99	3293.86	0.59	4.59	12.56
Rio Grande	150	37.19	71.68	130.87	0.60	1.71	3.60
Ganges-Brahmaputra	224	45.04	6945.60	17844.50	0.43	4.26	11.25
Upper Mississippi (gridded)	12788[a]	515.00	1410.37	3094.03	1.01	3.72	12.74

[a]When extracted every 5 m from gridded bathymetric data set.

methods for estimating d. We assume that h refers to geodetic water elevation above sea level. Cross-sections near bridges or dams were excluded from subsequent analysis. These values of w, W_e, and h, treated as error-free synthetic SWOT retrievals for the purposes of this analysis, were generated as follows.

[17] For each of the 1495 cross-sections, values of w and h were extracted at different channel depths, corresponding to percentages of bankfull mean depth d_{bf} ranging from 100% to 5% in increments of 5%. d_{bf} was visually determined at each cross-section by selecting the highest surveyed elevation that could be confidently determined as in-channel. At locations where multiple channels were encountered along the same surveyed transect (primarily the anastomosing Ganges-Brahmaputra river system) all channels were treated as a single cross-section. These derived pairs of w and h allow for exploration of w-h relationships as a function of percentage "channel exposure", i.e., the percentage of the channel area lying above the waterline for a given h.

[18] To estimate the probability that a required quantity of channel exposure might actually occur at least once during a nominal satellite mission lifetime (e.g., 3 years for SWOT), a second data set of synthetic w-h pairs was generated using HEC-RAS, to simulate river discharges along the Rio Grande and Upper Mississippi rivers. The necessary inputs and calibration parameters for these particular river reaches were previously defined by their respective developers [*Tetra Tech Inc*., 2005; *U.S. Army Corps of Engineers*, 2004]. For the Upper Mississippi River, this modeling was restricted to the downstream 430 of 639 cross-sections, owing to excessive influence of man-made structures on the HEC-RAS simulations. For each river, steady-state discharges ranging from 99% to 40% exceedance probability (the percentage of time that a given discharge is exceeded based on historic streamflow records) were simulated and the corresponding values of w, h, and d extracted from the surveyed cross-sections. These exceedance probabilities were determined using 10 years (2001–2010) of daily discharge records from four USGS gaging stations along the Upper Mississippi River and one along the Rio Grande River (Figure 1). A 99% exceedance probability roughly corresponds with the lowest magnitude discharge, and thus the greatest percentage of channel exposure, that could potentially be encountered over a mission lifetime, while a 40% exceedance probability roughly corresponds with the highest magnitude discharge that remains in-channel at all cross-sections along each river. Thus, the channel exposure percentages corresponding with these exceedance probabilities are unique to each cross-section, and range from nearly 100% channel exposure in some locations (at 99% exceedance probability) to nearly 0% channel exposure (at 40% exceedance probability).

[19] To study the effects of reach-averaging on remotely sensed hydraulic relationships, synthetic values of W_e and reach-averaged h were extracted from the gridded Upper Mississippi bathymetric data set as follows. First, these data were discretized into 12,788 5 m sections using the USACE HEC-GeoRAS extension for ArcGIS®. Each section thus represents the average bathymetry for the shortest possible reach length (5 m) permitted by this high-resolution data set. Synthetic pairs of W_e and h were then extracted from all 12,788 sections in much the same manner as for the cross-section database, except the reference d_{bf} was defined as the highest recorded elevation for each section instead of from visual inspection (unlike the surveyed cross-sections, the bathymetric data do not extend onto the river floodplain). Synthetic pairs of W_e and h were extracted from each section at water levels corresponding to percentages of d_{bf} ranging from 100% to 5%, then spatially averaged for reach-lengths of 50, 100, 500, 1000, 2000, 3000, 4000, 5000, 6000, 7000, 8000, 9000, and 10,000 m. The mathematical mean of h (for a given percentage of d_{bf}) was taken from all cross-sections within a given spatial-averaging length. The spatial-averaging "window" was then shifted 5 m and the mean taken again. Thus, fewer reach-averaged sections were extracted as reach-averaging length increased. Unlike traditional surveyed cross-sections, these synthetic, reach-averaged W_e and h values derived from a continuous bathymetric data set enable assessment of how spatial averaging of remotely sensed observations may influence hydraulic W_e-h relationships in natural river systems.

2.3. Linear Method for Depth Estimation

[20] The simplest approach to estimating mean flow depth below some lowest observed water level ($h_{\min}$) seeks river locations with a strongly linear relationship between all pairs of w (or W_e) and h lying above $h_{\min}$, and assumes this relationship may be extrapolated below that level down to w=0 to obtain $z_{\min}$ (e.g., Figure 2, top row).

[21] To implement this, the derivatives (approximated by finite forward differences) of h with respect to w ($\mathrm{d}h/\mathrm{d}w$) were first calculated between all simulated in-channel water surfaces (i.e., between each two adjacent water surfaces) above a given $h_{\min}$ for each cross-section in the compiled database. Those cross-sections where all observed values of $\mathrm{d}h/\mathrm{d}w$ were within ± 0.015 of each other were flagged. This value was determined from trial-and-error so as to select for locations with strong w-h relationships

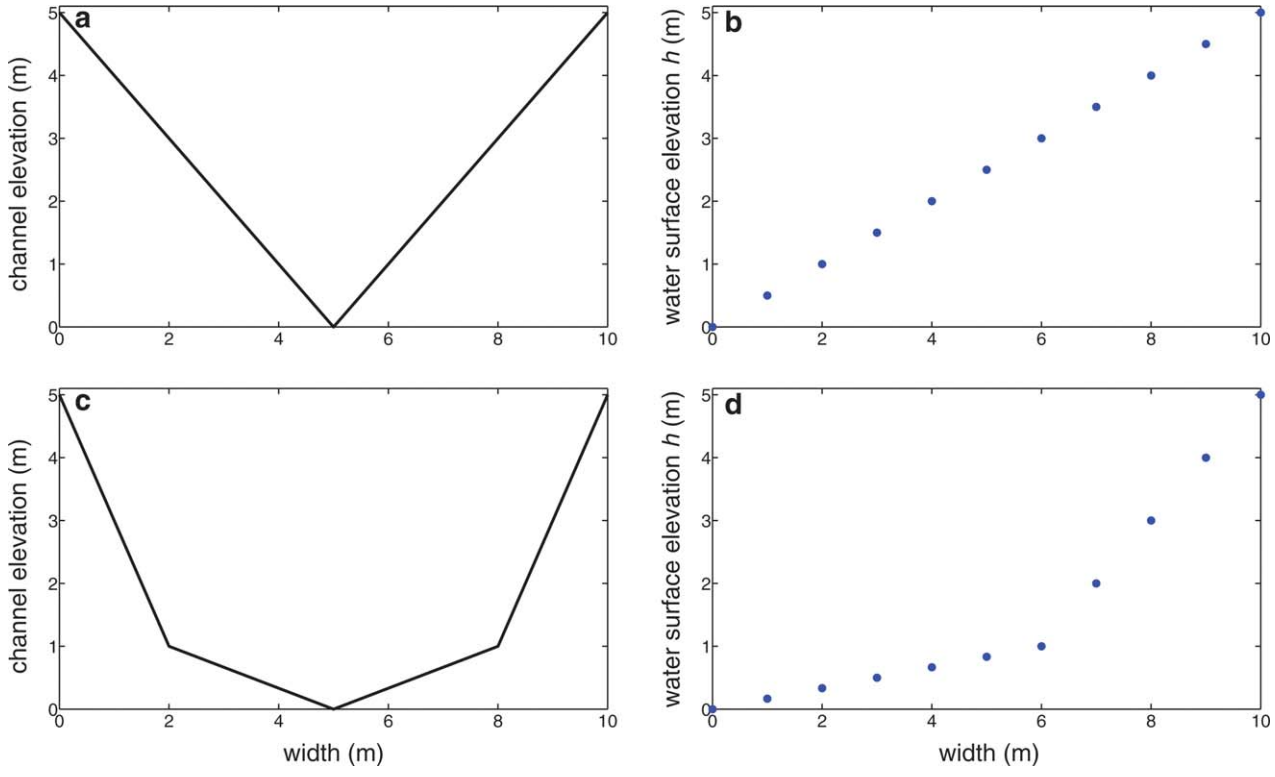

Figure 2. (a and c) Two conceptual, idealized river bathymetric cross-sections and (b and d) their respective plots of w versus h for a range of hypothetical flow levels. A single linear w-h relationship (Figure 2b) exists for cross-section (Figure 2a), whereas two linear relationships, one for moderate to high flows and one for low flows (Figure 2d) exist for cross-section (Figure 2c).

while still retaining a sufficient number of cross-sections from the sample pool for which to estimate depth. For all locations satisfying this criterion (called "optimal" locations), the mean of the derivatives of h with respect to w ($\overline{\mathrm{d}h/\mathrm{d}w}$) for all water surfaces above $h_{\min}$ was extrapolated to compute the minimum channel elevation ($z_{\min}$), the elevation for w=0. Next, $z_{\min}$ was subtracted from $h_{\min}$ to compute the maximum channel depth ($d_{\max}$) then halved to compute an estimate of d (d_{est}) (given the perfectly linear relationship between width and h that this method assumes, $d_{\mathrm{est}} = d_{\max}/2$ for any given h). An example of an optimal location detected by the Linear Method is displayed in Figure 3 (top).

[22] The Linear Method was tested for all cross-sections in the compiled database. For those cross-sections satisfying the algorithm's requirements (optimal locations), the resultant depth estimates d_{est} were compared with true d (for a given $h_{\min}$) to assess the accuracy of the approach. This process was repeated for a range of possible $h_{\min}$ values (i.e., from 80% to 5% of d_{bf}), to assess performance of the Linear Method from low- to high-channel bathymetry exposure.

2.4. Slope-Break Method for Depth Estimation

[23] An obvious limitation of the Linear Method is that hydraulic relationships determined at moderate to high flows are often inappropriate for low flows, owing to the presence of HG "slope breaks" as described earlier [*Lewis*, 1966]. This suggests that restricting the described linear extrapolation to a low-flow width-h relationship, if one can be discerned, may improve the derived estimates of $z_{\min}$ and d_{est}. To test this idea, a second depth-estimation algorithm was developed that selects for slope-break locations only where a second, distinct low-flow width-h relationship can also be detected, which is then extrapolated as before to estimate $z_{\min}$ and d_{est}. As such, this method seeks particular locations where two stable width-h relationships are found instead of one (e.g., Figure 2, bottom). The term "slope break" refers to the break in slope of a line fit through a scatterplot of h versus w (or W_e) at locations where this requirement is met (e.g., Figure 3, bottom). This slope break defines the h at which the set of hydraulic relationships defined for moderate to high flows is replaced by a new set of hydraulic relationships defined for low flows.

[24] For every cross-section (or reach-averaged section, for continuously gridded W_e) for each river, $\mathrm{d}h/\mathrm{d}w$ was first calculated for all synthetic water surfaces above a given $h_{\min}$ (i.e., between each two adjacent water surfaces), as for the Linear Method. $\overline{\mathrm{d}h/\mathrm{d}w}$ was calculated from the four highest water surfaces at each cross-section (the number of observations for calculating $\mathrm{d}h/\mathrm{d}w$ was arbitrarily chosen; this value had little effect on the results) and was then used to compare each subsequent (i.e., at lower elevation) value of $\mathrm{d}h/\mathrm{d}w$. If a subsequent value of $\mathrm{d}h/\mathrm{d}w$ deviated sufficiently from $\overline{\mathrm{d}h/\mathrm{d}w}$ (a $\mathrm{d}h/\mathrm{d}w$ value $<0.3^{*}\overline{\mathrm{d}h/\mathrm{d}w}$), the cross-section was flagged as having a slope break. Otherwise, $\overline{\mathrm{d}h/\mathrm{d}w}$ was recalculated to include the subsequent value of $\mathrm{d}h/\mathrm{d}w$ and the process continued until all values were compared. Note that the value 0.3, which defines the threshold for what constitutes a slope break, was chosen

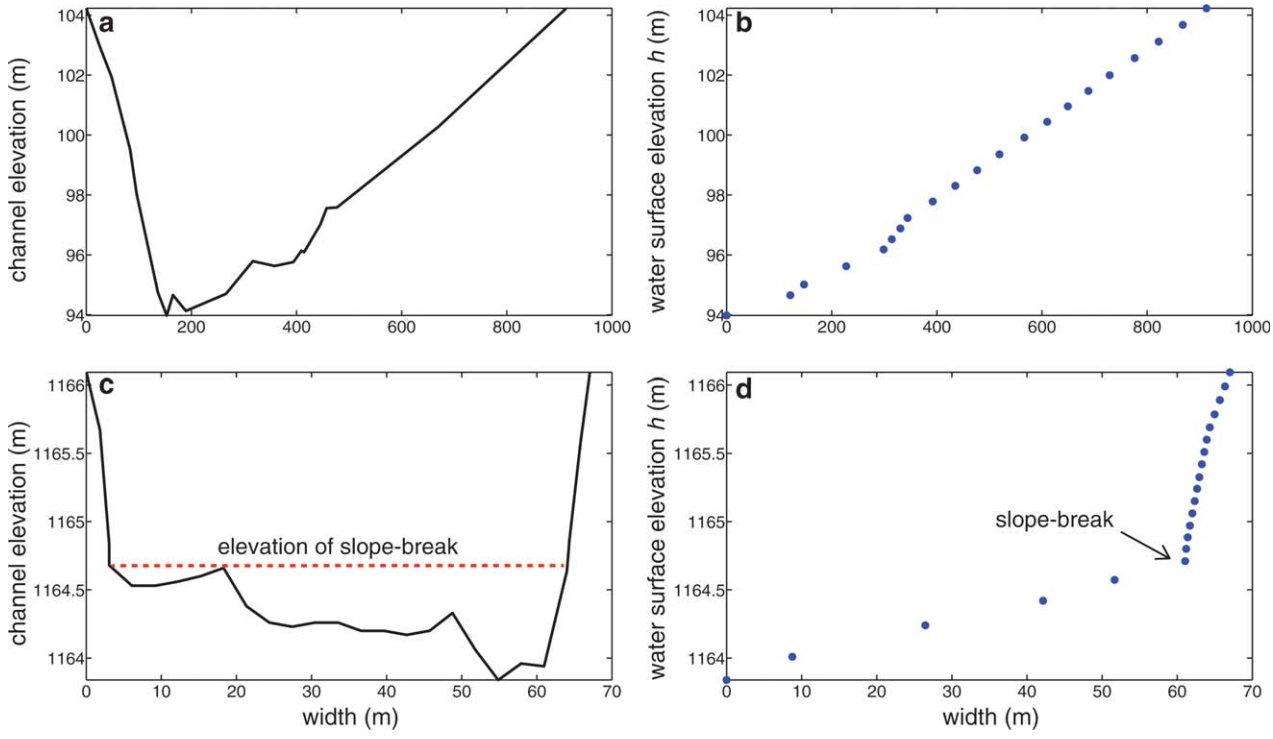

Figure 3. Examples of two field-surveyed cross-sections (a and c) identified as "optimal" by the Linear and Slope-Break methods, respectively. For cross-section (Figure 3a) the in-channel *w*-*h* relationship (Figure 3b) remains strongly linear with depth, and would thus be suitable for remote estimation of z_{min} and d based on remotely sensed observations of w and h alone using the Linear Method. In contrast, the channel geometry of cross-section (Figure 3c) yields a *w*-*h* plot (Figure 3d) with two distinct linear relationships, one for moderate to high flows and one for low flows. If water levels drop sufficiently such that the slope-break becomes observable by satellite (>70% channel exposure required, for this particular cross-section), the low-flow *w*-*h* relationship may be usefully extrapolated using the Slope-Break Method to estimate z_{min} and d based on remotely sensed observations of w and h alone.

through simple trial and error, but the value of this threshold did not have much effect on results. For cross-sections where a slope break was detected, d_{est} was only estimated at those locations where all values of dh/dw below the slope break and above h_{min} remained consistent with each other (i.e., within ± 0.015, as for the Linear Method). Extrapolation of $\overline{dh/dw}$ to $w = 0$ below this break was then used to estimate z_{min} and d_{est} as before. An example of an optimal location detected by the Linear Method is displayed in Figure 3 (bottom).

[25] The Slope-Break Method was tested for all cross-sections in the compiled database. For those cross-sections satisfying the algorithm's criteria (optimal locations) resultant values of d_{est} were compared with true d (for a given h_{min}) to assess the accuracy of this approach. As with the Linear Method, this process was repeated for a range of possible h_{min} values (i.e., from 80% to 5% of d_{bf}), to assess how width-*h* relationships might vary as a function of river channel exposure. Results were compared with those of the Linear Method for each river (Figure 6). This initial comparison of the two methods made clear that the Slope-Break Method outperformed the Linear Method for all rivers, thus further testing was limited to the Slope-Break Method alone. The Slope-Break Method was further tested on HEC-RAS-generated water surface profiles for reaches of the Rio Grande and Upper Mississippi rivers. Finally, the Slope-Break Method was tested on synthetic measurements extracted from the Upper Mississippi gridded bathymetric data set for a range of reach-averaging length scales.

3. Results

3.1. Depth Estimates at Channel Cross-Sections Using the Linear Method

[26] Standard and root mean squared errors (RMSEs) for mean depth retrievals estimated using the Linear Method are shown in Figure 4, varying as a function of percent channel exposure. Each blue symbol represents the standard error of the derived d_{est} (percent error relative to d_{bf}) at any location deemed optimal (i.e., having a single strongly linear *w*-*h* relationship) for a given channel exposure. Algorithm performance is highly site specific, with standard errors in depth retrieval varying several orders of magnitude regardless of channel exposure (blue symbols, Figure 4). Viewed collectively, the RMSE values (red symbols) for cross-section exposures ranging from 95% (high exposure) to 20% (low exposure) for all optimal locations detected range from 11% to 302%, 18% to 377%, 760% to 1288%, and 7% to 109% for the Upper Mississippi, Illinois, Rio Grande, and Ganges-Brahmaputra river systems, respectively. Both the

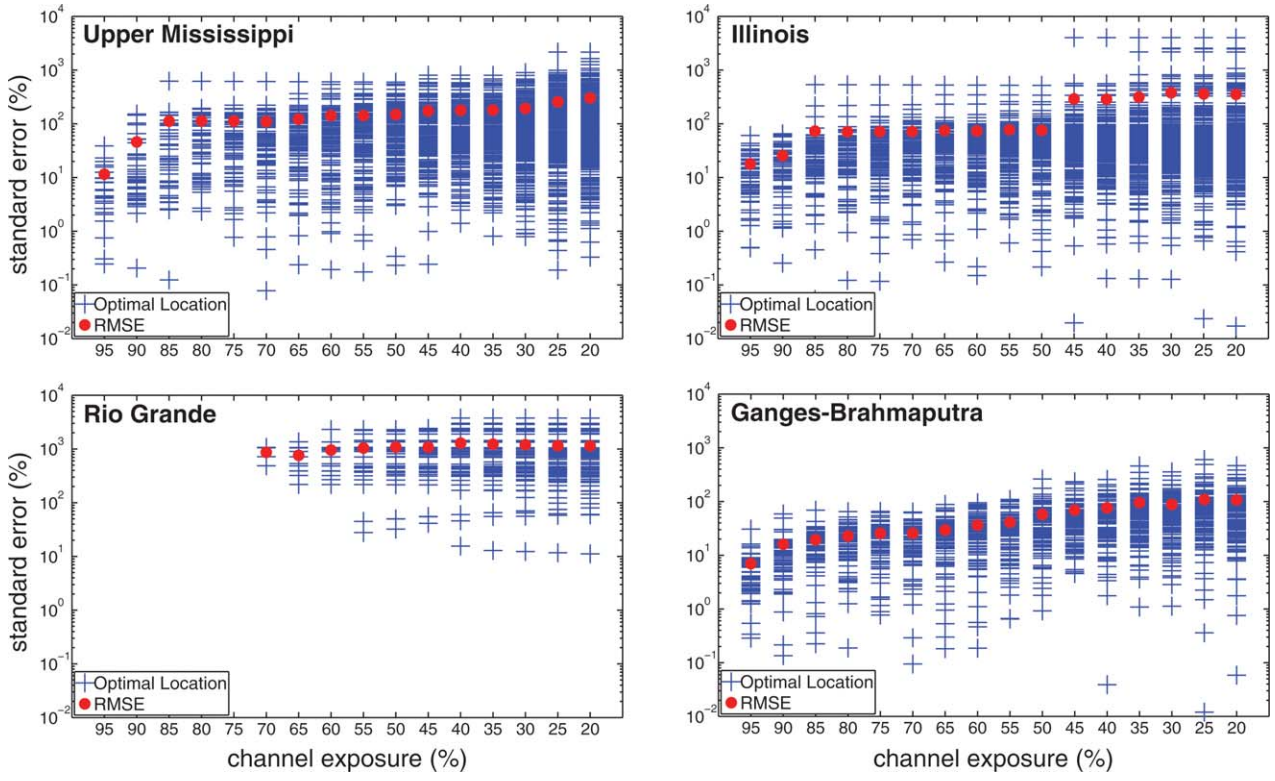

Figure 4. Standard and RMS errors for "optimal" locations for remote depth estimation, identified by applying the Linear Method to synthetic values of w and h extracted from 1495 cross-sections from four river systems. Errors are generally high (note log-normal scale). Each blue plus symbol represents the standard error (percent error in d_{est} relative to d_{bf}) for a single optimal location detected for a given percentage of channel exposure. The RMSE for all estimates for a given percentage of channel exposure is plotted in red. In all four river systems, errors tend to improve but the total number of optimal locations detected tends to decrease with increasing channel exposure. Note that for the Rio Grande, no optimal locations are detected when channel exposure exceeds ~70%.

RMSE values and the number of optimal locations detected tend to decrease with increasing channel exposure for all four river systems (the reasons for this are discussed in section 4). For example, at 20% channel exposure 942 (63%) of the total 1495 cross-sections were detected as optimal locations, while only 166 (11%) were detected as optimal at 95% channel exposure. At least some optimal locations were detected for all levels of channel exposure (20%–95%) in all rivers except the Rio Grande, where no optimal locations were detected at levels of channel exposure >70%.

3.2. Depth Estimates at Channel Cross-Sections Using the Slope-Break Method

[27] Standard and RMS errors for mean depth retrievals estimated using the Slope-Break Method are shown in Figure 5, varying as a function of percent channel exposure. Viewed collectively, the RMSE values (red symbols) for cross-section exposures ranging from 95% (high exposure) to 20% (low exposure) for all optimal locations detected range from 3% to 20%, 4% to 35%, 2% to 8%, and 4% to 65%, for the Upper Mississippi, Illinois, Rio Grande, and Ganges-Brahmaputra river systems, respectively. There is a sharp reduction in both RMSE values and the range of d_{est} errors for a given percentage of channel exposure produced by the Slope-Break Method (Figure 5) as compared with the Linear Method (Figure 4). As with the Linear Method, RMSE values tend to improve with increasing channel exposure for all four river systems, but in contrast to the Linear Method, the number of optimal locations detected tends to increase with increasing channel exposure for the Slope-Break Method (Figure 6; the reasons for this are discussed in section 4). For example, at 20% channel exposure only 6 (0.4%) of the 1495 cross-sections were detected as optimal locations, whereas 242 (16%) were detected as optimal locations at 95% channel exposure. Optimal locations were detected at all levels of channel exposure (20%–95%) for both the Upper Mississippi and Ganges-Brahmaputra rivers and at levels of channel exposure ≥30% for the Illinois River, but ≥80% channel exposure was required to detect optimal locations along the Rio Grande River.

3.3. Depth Estimates at Channel Cross-Sections Using the Slope-Break Method and Water Surface Profiles Simulated From HEC-RAS

[28] To exploit the described slope breaks in w-h relationships, water levels must fall to the required level of channel exposure and be imaged at least once during a satellite mission lifetime. To assess how probable this occurrence might

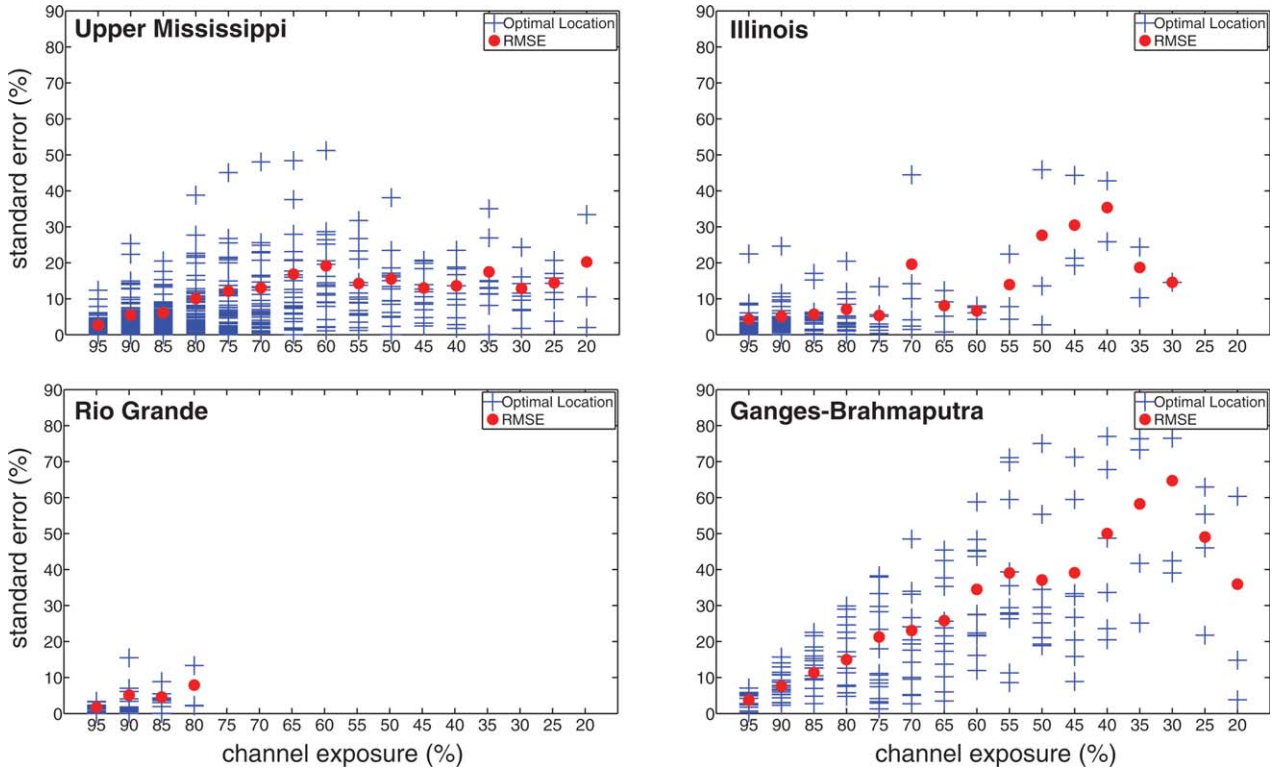

Figure 5. Standard and RMS errors for "optimal" locations for remote depth estimation, identified by applying the Slope-break Method to synthetic values of w and h extracted from 1495 cross-sections from four river systems. Note use of normal scale and significantly reduced errors relative to Figure 4. Each blue plus symbol represents the standard error (percent error in d_{est} relative to d_{bf}) at a single optimal location detected for a given percentage of channel exposure. The RMSE for all estimates for a given percentage of channel exposure is plotted in red. In all four river systems, errors tend to improve and the total number of optimal locations detected also tends to increase with increasing channel exposure. Note that for the Illinois and Rio Grande, no optimal locations are detected when channel exposure is less than ~30% and ~80%, respectively.

be, HEC-RAS simulations of water surface profiles were produced for the Upper Mississippi and Rio Grande rivers given their historic discharge statistics from USGS gaging stations. Standard and RMSE for d_{est} retrievals estimated using the Slope-Break Method on HEC-RAS water surface profile simulations are shown in Figure 7, varying as a function of discharge exceedance probability. Using the Upper Mississippi as an example, at 40% exceedance probability (meaning that this magnitude of discharge is exceeded 40% of the time, and thus this level of channel exposure (or greater), occurs roughly 60% of the time), 14 of the 430 cross-sections tested meet the criteria as optimal slope-break locations, with a RMSE of 22.95% relative to d_{bf}. Viewed collectively, the standard errors in depth retrievals range from 0.08% to 86% and 0.01% to 3.60% for the Upper Mississippi and Rio Grande rivers, respectively. The RMSE values for exceedance probabilities ranging from 99% (high exposure) to 40% (low exposure) for all optimal locations detected range from 20% to 31% and 0.75% to 2.25% for the Upper Mississippi and Rio Grande rivers, respectively. While RMSE values tend to decrease with increasing exceedance probability (corresponding to increasing channel exposure) for the Rio Grande, a slight trend of increasing RMSE values with increasing exceedance probability is found for the Upper Mississippi. Optimal locations were detected along the Upper Mississippi for all tested exceedance probabilities (40–99%), while only for exceedance probabilities ≥58% for the Rio Grande River. As with previous tests using the Slope-Break Method, the number of optimal locations detected tends to increase with increasing channel exposure for both rivers. For the Rio Grande, while only 2 (1.3%) of the 150 cross-sections were detected at 58% exceedance probability, 6 (4.0%) were detected at 90% exceedance probability. For the Upper Mississippi, 14 (3.3%) of 430 cross-sections were detected as optimal locations at 40% exceedance probability, while 42 (9.8%) were detected at 99% exceedance probability.

3.4. Depth Estimates for River Reaches Using the Slope-Break Method and Reach-Averaged Effective Width W_e and h

[29] Unlike intermittent cross-sections, the continuously gridded bathymetric data set for the Upper Mississippi River enables assessment of how reach-averaging (spatial-averaging) of continuous measurements of W_e and h may influence the quality of the obtained d_{est} retrievals. Standard and RMS errors for d_{est} retrievals estimated using the Slope-Break Method on reach-averaged W_e and h are shown

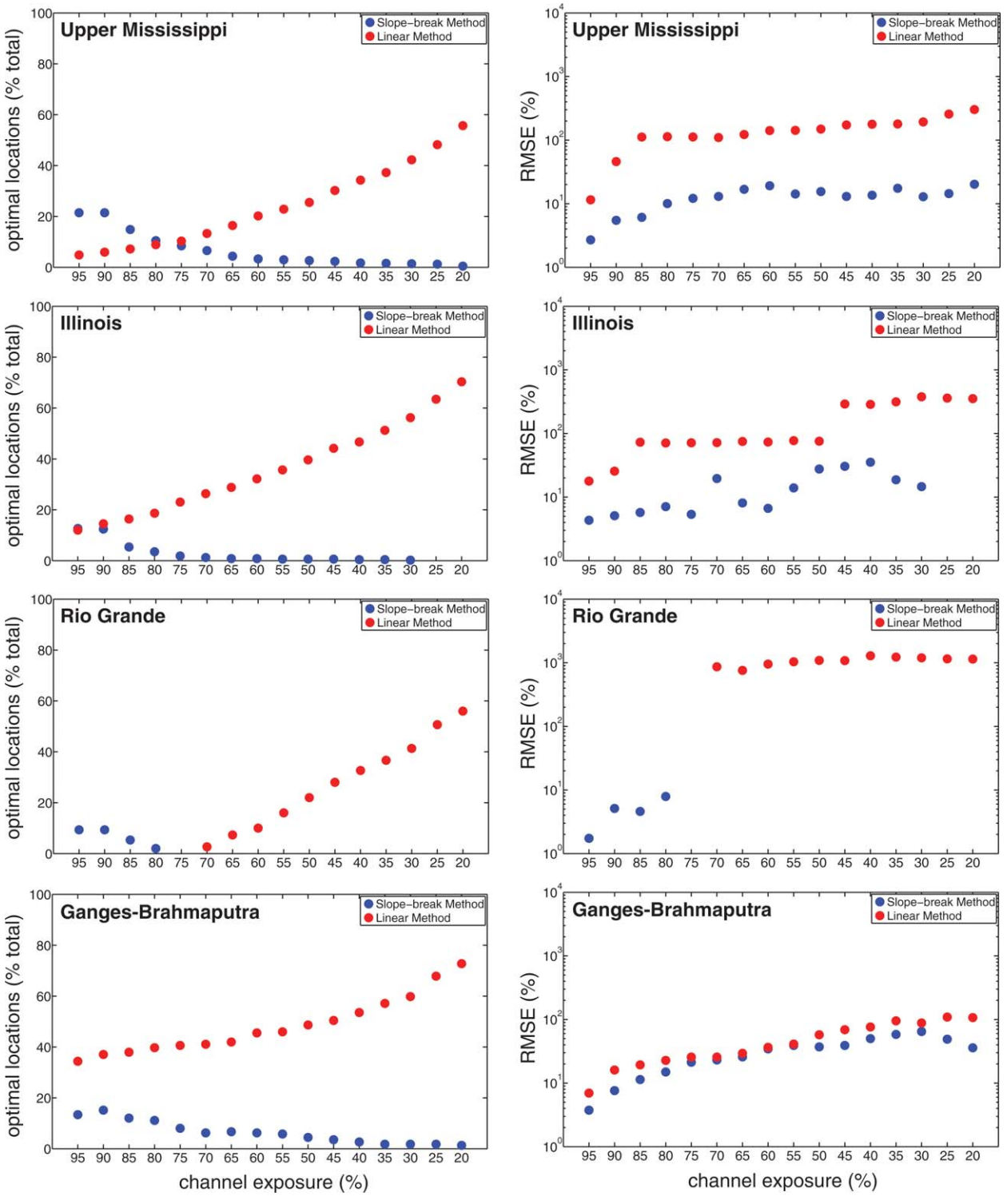

Figure 6. Comparison of the percentage of cross-sections detected as optimal (left column), and their corresponding RMSE values (calculated from the percent error in d_{est} relative to d_{bf}, for all estimates for a given percentage of channel exposure) (right column) for the Linear Method (red) and Slope-Break Method (blue) for each of the four river systems studied. Note the opposing trends in the number of optimal locations detected by each method, and the superior performance of the Slope-Break Method across all levels of channel exposure.

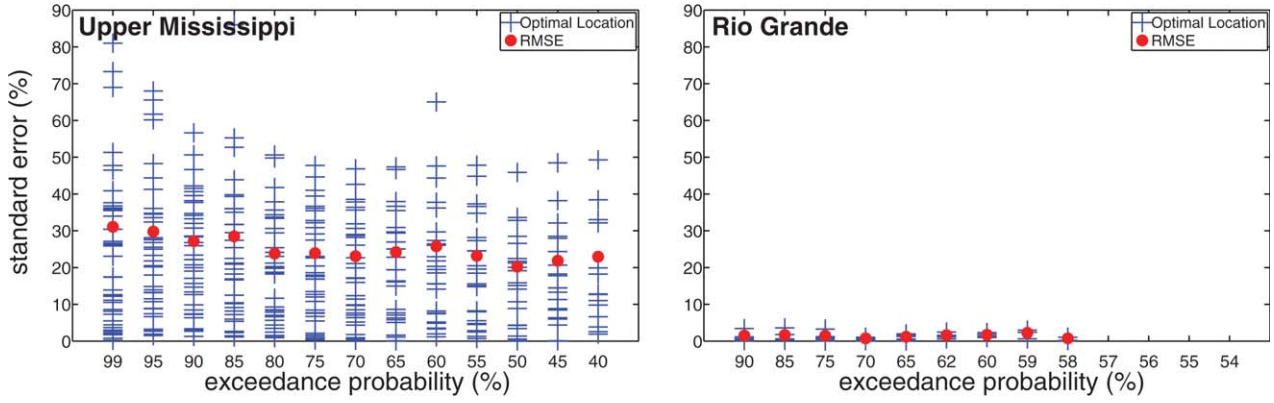

Figure 7. Standard and RMS errors for optimal locations identified by applying the Slope-break Method to simulated water surface elevations (h) modeled in HEC-RAS for a range of discharge exceedance probabilities (the percentage of time that a given discharge is exceeded, based on historic streamflow records) along the Upper Mississippi and Rio Grande Rivers. Each blue plus symbol represents the standard error (percent error in d_{est} relative to d_{bf}) for a single optimal location detected for a given discharge exceedance probability. The RMSE for all estimates for a given exceedance probability is plotted in red. Useful slope-breaks are detected at flow levels which are exceeded ~40% and ~58% of the time for the Upper Mississippi and Rio Grande rivers, respectively (thus indicating that adequate channel exposures occur roughly 60% and 42% of the time, respectively.

in Figure 8, varying as a function of percent channel exposure as before. A summary comparison of how these errors vary with reach-averaging length is plotted in Figure 9. As for the slope-break analysis based on cross-sections, both RMSE values and the range of errors for reach-averaged sections tend to decrease with increasing channel exposure for those reaches where slope breaks were detected. Likewise, the number of optimal locations for a given reach-averaging length tends to increase with increasing channel exposure, as shown in Figure 9. However, as reach-averaging length increases, the number of optimal locations for a given percentage of channel exposure decreases, and a greater percentage of channel exposure is required in order for optimal slope breaks to be detected. RMSE values for a given percentage of channel exposure remain relatively consistent at all reach-averaging lengths up to ~2000 m, but tend to increase somewhat at longer lengths. Optimal slope-breaks were not detected at any level of channel exposure for reach-averaging lengths exceeding ~7000 m. However, between reach-averaging lengths of 5 m and 7000 m the range of errors for all optimal locations detected for a given percentage of channel exposure tends to decrease as reach-averaging length scale is increased. The reasons for this are discussed next.

4. Discussion and Conclusions

[30] The findings of this study suggest that remotely sensed measurements of river cross-sectional or reach-averaged flow width (w or W_e) and water surface elevation h alone may be useful for estimating mean river depth d, at select locations, if a sufficient number of observations are accumulated over time so as to identify stable empirical relationships between the two variables. Because moderate-to high-flow hydraulic relationships often do not extend to low flows, a sufficient portion of a river channel's bathymetry must be observed (i.e., h must fall to sufficiently low levels) in order to identify hydraulic relationships that may usefully be extrapolated to estimate depth. The minimum amount of channel exposure necessary for the method to work varies between rivers and for different locations along the same river. While the variability in required channel exposure is likely due to in part to the different geometries and hydrologic regimes of the rivers studied, this finding is also potentially related to the limited sample sizes of the cross-sectional and bathymetric data sets used.

[31] Testing of the Linear Method, for example, shows that a simple linear extrapolation of w-h relationships observed at moderate to high flow levels can lead to wildly inaccurate depth estimates (Figure 4). In contrast, testing of the Slope-Break Method suggests that extrapolation of low-flow w-h relationships at those locations where a second linear relationship is found can substantially reduce this error. Indeed, as compared to the Linear Method the Slope-Break Method demonstrates superior performance in flow depth estimation for all four rivers at all levels of channel exposure (Figure 6). Although the Linear Method technically detects a greater number of "optimal" locations, with less channel exposure, as compared with the Slope-Break Method, this seeming benefit is offset by considerably larger errors in the derived depth estimates. Indeed, as channel exposure increases, the Linear Method detects *fewer* optimal locations, as many locations displaying "stable" w-h relationships at moderate to high flow levels are later revealed to have unstable w-h relationships if more of the channel is exposed (e.g., Figure 3, bottom row). While a small number of purely linear w-h relationships were preserved throughout the entire range of possible h values for the cross-sections studied here, such locations could not in practice be detected from space unless they became fully exposed (i.e., the river dries up) during at least one satellite overpass. Therefore, despite the Linear Method's apparent appeal of identifying numerous candidate locations with low amounts of channel exposure, its overly simplistic assumptions yield poor depth-estimation results.

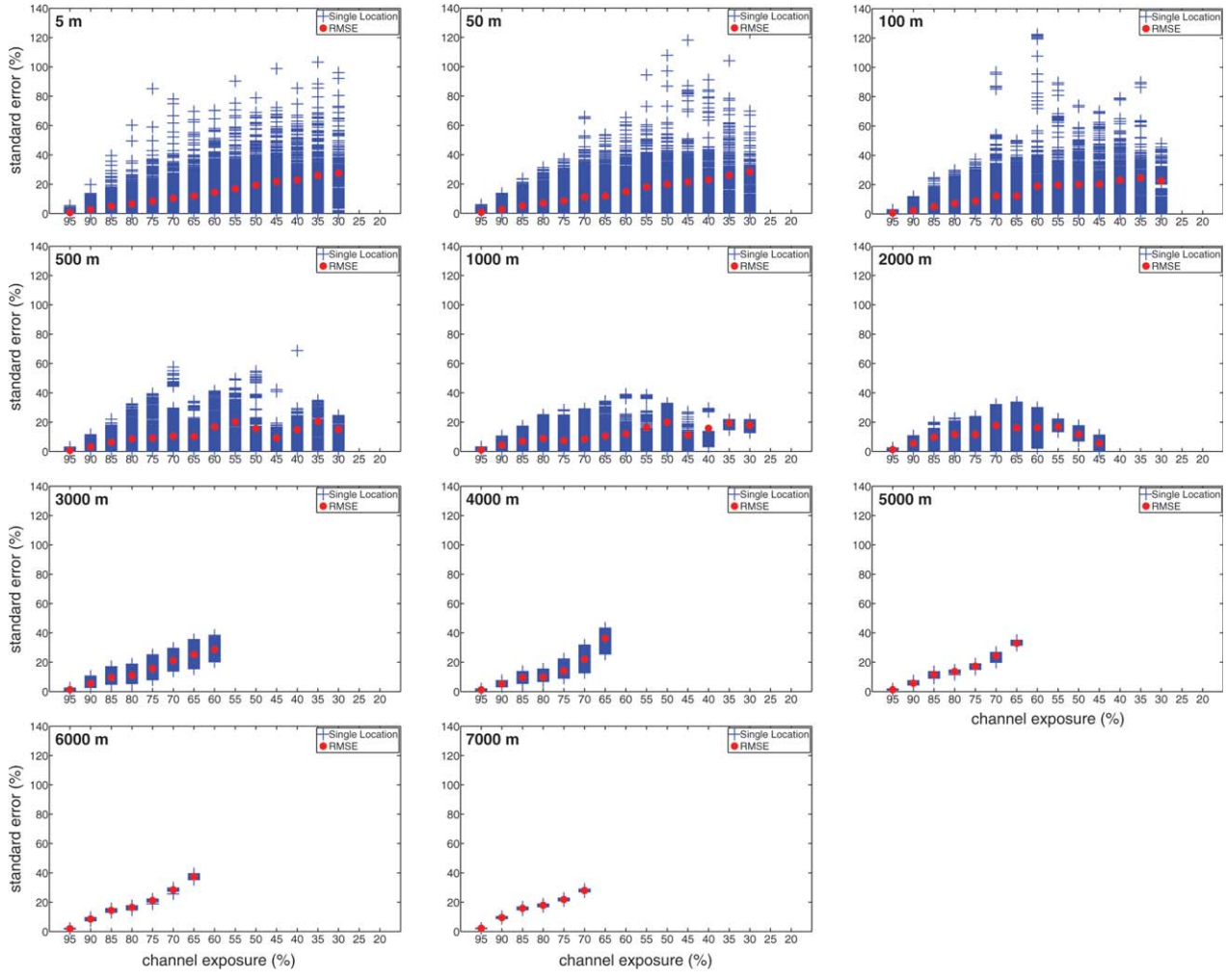

Figure 8. Standard and RMS errors for optimal locations for remote depth estimation, identified by applying the Slope-break Method to synthetic values of reach-averaged effective width W_e and h extracted from 62 km of continuously-gridded bathymetry along the Upper Mississippi. The level of spatial-averaging performed ranges from 5 m (native resolution) to 7 km river reach lengths. Each blue plus symbol represents the standard error (percent error in d_{est} relative to d_{bf}) at a single optimal location detected for a given percentage of channel exposure The RMSE for all estimates for a given percentage of channel exposure is plotted in red. For a given percentage of channel exposure, both depth retrieval errors and the total number of optimal locations identified decrease substantially with increasing reach-averaged length. For this particular river, a reach-averaged length of approximately 1000–2000 m strikes an optimal balance between improved quality of the depth-retrieval estimates and total number of optimal locations found.

[32] The Slope-Break Method mitigates this weakness by selecting for locations where two linear trends in the width-h relationship are detected instead of one. While still a simple model, this more closely reflects real-world channel geometries associated with cut banks and alluvial bar formation, as well as field-based geomorphic observations of high- versus low-flow hydraulic geometries [e.g., *Lewis*, 1966; *Richards*, 1976; *Jowett*, 1998]. This also plausibly explains why the Slope-Break Method, in contrast to the Linear Method, tends to detect more optimal locations as channel exposure increases, because as h falls and submerged slope breaks are revealed such locations become qualified for the former and disqualified for the latter. The detection of numerous slope breaks even with channel exposures as low as 20% (e.g., the Upper Mississippi and Ganges-Brahmaputra river systems, Figure 5), is somewhat surprising given that slope breaks were initially assumed to occur only at low-flow h values. Nonetheless, the overall conclusion to be drawn is that the Slope-Break Method detects fewer optimal locations than the Linear Method, but offers substantially smaller errors.

[33] Even for the Slope-Break Method, substantial, site-specific errors remain if the method is applied to the scale of traditional surveyed cross-sections, long known to vary greatly from one place to the next along natural river systems [e.g., *Leopold and Maddock*, 1953; *Richards*, 1973; *Knighton*, 1975; *Park*, 1977]. In contrast, longitudinal reach-averaging of W_e and h substantially reduces uncertainty in the obtained depth estimates (Figure 8). As such, reach-averaging does not appear to diminish the quality of observed empirical hydraulic relationships, and may actually

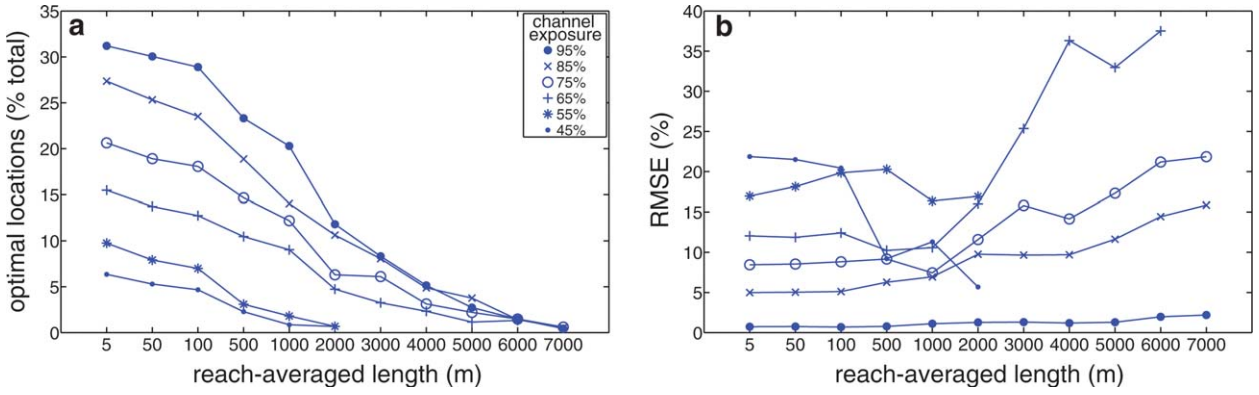

Figure 9. Comparison of (a) the percentage of reaches detected as optimal locations by the Slope-Break Method; and (b) their corresponding RMSE values (calculated from the percent error in d_{est} relative to d_{bf}, for all estimates for a given percentage of channel exposure), both varying with reach-averaged length and percentage of channel exposure. The number of optimal cross-sections identified generally increases with channel exposure but decreases with increasing reach-averaging length. RMSE values for d_{est} tend to decrease with increasing channel exposure and remain fairly consistent for reach-averaged lengths between 5 m and 2000 m, but degrade at longer reach-averaged lengths.

improve their robustness through spatial-averaging of local geomorphic heterogeneities. Therefore, while increased reach-averaging tends to reduce the total number of optimal locations detected, the quality of the derived depth estimate is improved, at least for the Upper Mississippi data set tested here (Figure 8). For this particular river, a high-quality depth retrieval is ensured using reach lengths of ~1000 to 2000 m, which is roughly 2–3 times mean bankfull channel width. This finding agrees with *Smith and Pavelsky* [2008], who found that remotely sensed HG *b*-exponents reached stable values once reach-averaging lengths are increased to ~2–3 times river floodplain width.

[34] This finding of improved depth estimation through greater reach-averaging of observed hydraulic variables is especially promising in the SWOT context, given its technological requirement to spatially average raw native-resolution radar echoes to improve the measurement precision of its h measurement. Although examining the impact of SWOT measurement precision on the conceptual depth estimation technique presented here lies beyond the scope of this study, like all radars SWOT measurement precision is improved through increased spatial-averaging, an approach compatible with river reach-averaging. Furthermore, the exceedance probability simulations presented in Figure 7 suggest that the temporal sampling of SWOT and other satellites is more than adequate to encounter the required exposures of channel bathymetry, with sufficiently low flows in the Upper Mississippi and Rio Grande rivers occurring at least ~60% and ~42% of the time, respectively.

[35] This study was limited by the availability and limitations of field-based data sets, and the predominant use of traditional surveyed cross-sections. Unlike imaging technologies, cross-sections provide only 2-D information, and only at intermittent locations. Even the continuous sonar bathymetric data set for the Upper Mississippi was somewhat removed from real-world conditions, owing to its removal of surface water slope dh/dx and lack of bankfull coverage. Future work should apply the methods developed herein to more realistic riverine measurements, e.g., measurements from AirSWOT, an airplane-mounted, SWOT-like sensor planned for first flights over the Sacramento River in 2013 (http://swot.jpl.nasa.gov/Airswot/)). While our approach requires no bathymetric or floodplain DEM, a thorough assessment of how SWOT (or other sensors) width and h measurement errors would propagate further uncertainty to the derived depth estimates is warranted. Finally, it is important to reiterate that neither the Linear nor Slope-Break method can possibly produce continuous depth estimates everywhere along a river. Instead, they seek out a small subset of ideal channel locations where simple, linear correlations exist between a river's flow width and mean flow depth.

[36] Despite these limitations, this study puts forth a first, purely empirical method for estimating river flow depth based solely on remotely sensed measurements of river water surface elevation h and effective width W_e using no ancillary data whatsoever. Even intermittent depth estimates at a subset of ideal channel locations along a given river reach could potentially be used to back-out depth estimates throughout the remaining portion of the reach (e.g., using hydraulic relationships developed at optimal locations to estimate depth elsewhere). Successfully applied, intermittent retrievals of mean flow depth could aid remote estimation of river discharge, either as inputs to the Manning equation-based slope-area method [*Dingman*, 1994] or data assimilation into hydrodynamic models. The simplicity of the Slope-Break Method is much of its appeal, offering potential value as a first-order depth estimator for global river studies from space.

[37] **Acknowledgments.** This research was funded by the NASA Physical Oceanography Program (grant NNX10AE96G), managed by Eric Lindstrom. In situ cross-section data for the Ganges-Brahmaputra river system was provided by Faissal Hossain (Tennessee Technical University) as part of a Memorandum of Understanding between the Institute of Water Modeling—Bangladesh and Tennessee Technical University. In situ cross-section data for the Rio Grande (surveyed by Tetra Tech Inc.) and for the Upper Mississippi and Illinois rivers (surveyed by the U.S. Army Corps of Engineers) was provided to the authors by Edward Beighley (FM Global). The continuous in situ bathymetric data set for the Upper Mississippi was provided by the USGS, as part of the Long Term Resource Monitoring Program. The authors thank Doug Alsdorf, Paul Bates, and one anonymous reviewer for their constructive feedback on this paper.

References

Alsdorf, D. E., J. M. Melack, T. Dunne, L. A. K. Mertes, L. L. Hess, and L. C. Smith (2000), Interferometric radar measurements of water level changes on the Amazon flood plain, *Nature*, *404*(6774), 174–177, doi:10.1038/35004560.

Alsdorf, D. E., L. C. Smith, and J. M. Melack (2001), Amazon floodplain water level changes measured with interferometric SIR-C radar, *IEEE Trans. Geosci. Remote Sens.*, *39*(2), 423–431, doi:10.1109/36.905250.

Alsdorf, D. E., E. Rodríguez, and D. P. Lettenmaier (2007a), Measuring surface water from space, *Rev. Geophys.*, *45*, RG2002, doi:10.1029/2006RG000197.

Alsdorf, D. E., P. Bates, J. Melack, M. Wilson, and T. Dunne (2007b), Spatial and temporal complexity of the Amazon flood measured from space, *Geophys. Res. Lett.*, *34*, L08402, doi:10.1029/2007GL029447.

Andreadis, K. M., E. A. Clark, D. P. Lettenmaier, and D. E. Alsdorf (2007), Prospects for river discharge and depth estimation through assimilation of swath-altimetry into a raster-based hydrodynamics model, *Geophys. Res. Lett.*, *34*, L10403, doi:10.1029/2007GL029721.

Biancamaria, S., et al. (2011), Assimilation of virtual wide swath altimetry to improve Arctic river modeling, *Remote Sens. Environ.*, *115*(2), 373–381, doi:10.1016/j.rse.2010.09.008.

Birkett, C. M. (1998), Contribution of the TOPEX NASA radar altimeter to the global monitoring of large rivers and wetlands, *Water Resour. Res.*, *34*(5), 1223–1239.

Birkett, C. M., and B. Beckley (2010), Investigating the performance of the Jason-2/OSTM radar altimeter over lakes and reservoirs, *Mar. Geod.*, *33*(S1), 204–238, doi:10.1080/01490419.2010.488983.

Birkett, C. M., L. A. K. Mertes, T. Dunne, M. H. Costa, and M. J. Jasinski (2002), Surface water dynamics in the Amazon Basin: Application of satellite radar altimetry, *J. Geophys. Res.*, *107*(D20), 8059–8080, doi:10.1029/2001JD000609.

Bjerklie, D. M. (2007), Estimating the bankfull velocity and discharge for rivers using remotely-sensed river morphology information, *J. Hydrol.*, *341*(3–4), 144–155, doi:10.1016/j.jhydrol.2007.04.011.

Brakenridge, G. R., S. V. Nghiem, E. Anderson, and S. Chien (2005), Space-based measurement of river runoff, *Eos Trans. AGU*, *86*(19), 185–188.

Calmant, S., F. Seyler, and J. Crétaux (2008), Monitoring continental surface waters by satellite altimetry, *Surv. Geophys.*, *29*(4), 247–269, doi:10.1007/s10712-008-9051-1.

Crétaux, J.-F., and C. Birkett (2006), Lake studies from satellite radar altimetry, *C. R. Geosci.*, *338*(14–15), 1098–1112, doi:10.1016/j.crte.2006.08.002.

Dingman, S. L. (1994), *Physical Hydrology*, 2nd ed., Prentice Hall, Upper Saddle River, N. J. [Available at: http://www.cce.uri.edu/cels/nrs/whl/Teaching/nrs592/2009/Class%203%20Wetland%20Riparian%20Biogeochemistry/Soil%20Hydrology%20Bckground%20Dingman.pdf, accessed 19 Sept. 2012.].

Durand, M., K. M. Andreadis, D. E. Alsdorf, D. P. Lettenmaier, D. Moller, and M. Wilson (2008), Estimation of bathymetric depth and slope from data assimilation of swath altimetry into a hydrodynamic model, *Geophys. Res. Lett.*, *35*, L20401, doi:10.1029/2008GL034150.

Durand, M., E. Rodriguez, D. E. Alsdorf, and M. Trigg (2010a), Estimating river depth from remote sensing swath interferometry measurements of river height, slope, and width, *IEEE J. Selec. Top. Appl. Earth Obs. Remote Sens.*, *3*(1), 20–31, doi:10.1109/JSTARS.2009.2033453.

Durand, M., L.-L. Fu, D. P. Lettenmaier, D. E. Alsdorf, E. Rodriguez, and D. Esteban-Fernandez (2010b), The surface water and ocean topography mission: Observing terrestrial surface water and oceanic submesoscale eddies, *Proc. IEEE*, *98*(5), 766–779, doi:10.1109/JPROC.2010.2043031.

Fonstad, M. A., and W. A. Marcus (2010), High resolution, basin extent observations and implications for understanding river form and process, *Earth Surf. Process. Landforms*, *35*(6), 680–698, doi:10.1002/esp.1969.

Frappart, F., F. Seyler, J.-M. Martinez, J. G. León, and A. Cazenave (2005), Floodplain water storage in the Negro River basin estimated from microwave remote sensing of inundation area and water levels, *Remote Sens. Environ.*, *99*(4), 387–399, doi:10.1016/j.rse.2005.08.016.

Jowett, I. G. (1998), Hydraulic geometry of New Zealand rivers and its use as a preliminary method of habitat assessment, *Reg. Rivers Res. Manage.*, *14*(5), 451–466, doi:10.1002/(SICI)1099-1646(1998090)14:5<451::AID-RRR512>3.0.CO;2-1.

Jung, H. C., and D. Alsdorf (2010), Repeat-pass multi-temporal interferometric SAR coherence variations with Amazon floodplain and lake habitats, *Int. J. Remote Sens.*, *31*(4), 881–901, doi:10.1080/01431160902902609.

Jung, H. C., et al. (2010), Characterization of complex fluvial systems using remote sensing of spatial and temporal water level variations in the Amazon, Congo, and Brahmaputra Rivers, *Earth Surf. Proc. Landforms*, *35*(3), 294–304, doi:10.1002/esp.1914.

Khan, S. I., et al. (2011), Satellite remote sensing and hydrologic modeling for flood inundation mapping in Lake Victoria basin: Implications for hydrologic prediction in ungauged basins, *IEEE Trans. Geosci. Remote Sens.*, *49*(1), 85–95, doi:10.1109/TGRS.2010.2057513.

Knighton, A. D. (1975), Variations in at-a-station hydraulic geometry, *Am. J. Sci.*, *275*(2), 186–218, doi:10.2475/ajs.275.2.186.

Koblinsky, C. J., R. T. Clarke, A. C. Brenner, and H. Frey (1993), Measurement of river level variations with satellite altimetry, *Water Resour. Res.*, *29*(6), 1839–1848, doi:10.1029/93WR00542.

Lee, H., R. E. Beighley, D. Alsdorf, H. C. Jung, C. K. Shum, J. Duan, J. Guo, D. Yamazaki, and K. Andreadis (2011), Characterization of terrestrial water dynamics in the Congo Basin using GRACE and satellite radar altimetry, *Remote Sens. Environ.*, *115*(12), 3530–3538, doi:10.1016/j.rse.2011.08.015.

Legleiter, C. J., and D. A. Roberts (2009), A forward image model for passive optical remote sensing of river bathymetry, *Remote Sens. Environ.*, *113*(5), 1025–1045, doi:10.1016/j.rse.2009.01.018.

Legleiter, C. J., D. A. Roberts, W. A. Marcus, and M. A. Fonstad (2004), Passive optical remote sensing of river channel morphology and in-stream habitat: Physical basis and feasibility, *Remote Sens. Environ.*, *93*(4), 493–510, doi:10.1016/j.rse.2004.07.019.

Legleiter, C. J., D. A. Roberts, and R. L. Lawrence (2009), Spectrally based remote sensing of river bathymetry, *Earth Surf. Proc. Landforms*, *34*(8), 1039–1059, doi:10.1002/esp.1787.

Leopold, L., and T. Maddock (1953), The hydraulic geometry of stream channels and some physiographic implications, *Geol. Surv. Prof. Paper.* [Available at: http://scholarworks.umass.edu/fishpassage_reports/252.].

Lewis, L. A. (1966), The adjustment of some hydraulic variables at discharges less than one cfs, *Prof. Geogr.*, *18*(4), 230–234, doi:10.1111/j.0033-0124.1966.00230.x.

Lu, Z., M. Crane, O.-I. Kwoun, C. Wells, C. Swarzenski, and R. Rykhus (2005), C-band radar observes water level change in swamp forests, *Eos Trans. AGU*, *86*(14), 141, doi:10.1029/2005EO140002.

Marcus, W. A., and M. A. Fonstad (2008), Optical remote mapping of rivers at sub-meter resolutions and watershed extents, *Earth Surf. Proc. Landforms*, *33*(1), 4–24, doi:10.1002/esp.1637.

Marcus, W. A., and M. A. Fonstad (2010), Remote sensing of rivers: The emergence of a subdiscipline in the river sciences, *Earth Surf. Proc. Landforms*, *35*(15), 1867–1872, doi:10.1002/esp.2094.

Papa, F., C. Prigent, F. Durand, and W. B. Rossow (2006), Wetland dynamics using a suite of satellite observations: A case study of application and evaluation for the Indian Subcontinent, *Geophys. Res. Lett.*, *33*, L08401, doi:10.1029/2006GL025767.

Park, C. C. (1977), World-wide variations in hydraulic geometry exponents of stream channels: An analysis and some observations, *J. Hydrol.*, *33*(1–2), 133–146, doi:10.1016/0022–1694(77)90103-2.

Phillips, J. D. (1990), The instability of hydraulic geometry, *Water Resour. Res.*, *26*(4), 739–744, doi:10.1029/WR026i004p00739.

Prigent, C., E. Matthews, F. Aires, and W. B. Rossow (2001), Remote sensing of global wetland dynamics with multiple satellite data sets, *Geophys. Res. Lett.*, *28*(24), 4631–4634, doi:10.1029/2001GL013263.

Richards, K. S. (1973), Hydraulic geometry and channel roughness; a nonlinear system, *Am. J. Sci.*, *273*(10), 877–896, doi:10.2475/ajs.273.10.877.

Richards, K. S. (1976), Complex width-discharge relations in natural river sections, *Geol. Soc. Am. Bull.*, *87*(2), 199–206, doi:10.1130/0016-7606(1976)87<199:CWRINR>2.0.CO;2.

Rogala, J. T. (1999), Bathymetry - Chapter 2 extracted from James T. Rogala, 1999. Methodologies employed for bathymetric mapping and sediment characterization as part of the Upper Mississippi River System Navigation Feasibility Study, ENV Rep. 13, Interim Report for the Upper Mississippi River—Illinois Waterway System Navigation Study; prepared for U.S. Geol. Surv., U.S. Army Eng. Dist., Rock Isl., St. Louis.

Shiklomanov, A. I., R. B. Lammers, and C. J. Vörösmarty (2002), Widespread decline in hydrological monitoring threatens Pan-Arctic Research, *Eos Trans. AGU*, *83*(2), 13, doi:10.1029/2002EO000007.

Smith, L. C. (1997), Satellite remote sensing of river inundation area, stage, and discharge: A review, *Hydrol. Process.*, *11*, 1427–1439, doi:10.1002/(SICI)1099-1085(199708)11:10<1427::AID-HYP473>3.3.CO;2-J.

Smith, L. C., and T. M. Pavelsky (2008), Estimation of river discharge, propagation speed, and hydraulic geometry from space: Lena River, Siberia, *Water Resour. Res.*, *44*, 03427, doi:10.1029/2007WR006133.

Smith, L. C., B. L. Isacks, R. R. Forster, A. L. Bloom, and I. Preuss (1995), Estimation of discharge from braided glacial rivers using ERS 1 synthetic aperture radar: First results, *Water Resour. Res.*, *31*, 1325–1330, doi:10.1029/95WR00145.

Smith, L. C., B. L. Isacks, A. L. Bloom, and A. B. Murray (1996), Estimation of discharge from three braided rivers using synthetic aperture radar satellite imagery: Potential application to ungaged basins, *Water Resour. Res.*, *32*(7), 2021–2034, doi:10.1029/96WR00752.

Stewardson, M. (2005), Hydraulic geometry of stream reaches, *J. Hydrol.*, *306*(1–4), 97–111, doi:10.1016/j.jhydrol.2004.09.004.

Stokstad, E. (1999), Scarcity of rain, stream gages threatens forecasts, *Science*, *285*(5431), 1199–1200, doi:10.1126/science.285.5431.1199.

Tetra Tech, Inc. (2005), *FLO-2D Model Development Below Caballo Dam URGWOM: Final Report on FLO-2D Model Development*, Tetra Tech Inc., Albuquerque, N. M.

U.S. Army Corps of Engineers (2004), Upper *Mississippi River System Flow Frequency Study: Final Report*, U. S. Army Corps of Eng., Rock Isl. Dist.

United Nations Educational, Scientific and Cultural Organization (2012), *The United Nations World Water Development report 4*, United Nations Educ., Sci. and Cult. Organ., Paris, France.

Vörösmarty, C. J. et al. (2010), Global threats to human water security and river biodiversity, *Nature*, *467*(7315), 555–561, doi:10.1038/nature09440.